Journal of
Materials Chemistry A

Accepted Manuscript

This article can be cited before page numbers have been issued, to do this please use: G. Liu, Y. Wang, C. Shen, Z. Ju and D. Yuan, *J. Mater. Chem. A*, 2014, DOI: 10.1039/C4TA05349D.

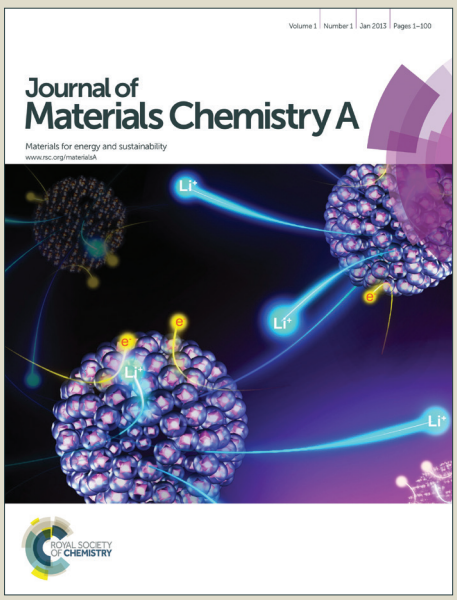

ROYAL SOCIETY OF CHEMISTRY

www.rsc.org/materialsA

Journal Name

RSCPublishing

View Article Online
DOI: 10.1039/C4TA05349D

ARTICLE

A facile synthesis of microporous organic polymers for efficient gas storage and separation

Cite this: DOI: 10.1039/x0xx00000x

Guoliang Liu,[a,b] Yangxin Wang,[a,b] Chaojun Shen,[a] Zhanfeng Ju[a] and Daqiang Yuan[*,a]

Received 00th January 2012,
Accepted 00th January 2012

DOI: 10.1039/x0xx00000x

www.rsc.org/

A series of porous hyper-cross-linked polymers with excellent physiochemical stability have been designed and prepared facilely through template-free Friedel-Crafts alkylation reactions between benzene / biphenyl / 1,3,5-triphenylbenzene as co-condensing rigid aromatic building blocks and 1,3,5-tris(bromomethyl)benzene or 1,3,5-tris(bromomethyl)-2,4,6-trimehylbenzene as cross-linkers under the catalysis of anhydrous $AlCl_3$ or $FeCl_3$. The systematic study of gas uptake ability shows that anhydrous $AlCl_3$ is a much more effective catalyst than anhydrous $FeCl_3$. The synthesized polymers are thermally stable and are predominantly microporous with high surface areas up to 1783 m^2g^{-1}. In addition, they exhibit high H_2 and CO_2 uptake capacity/selectivity. Among these materials, **C1M3-Al** has the highest H_2 uptake capacity at 77 K and 1 bar (19.1 $mg{\cdot}g^{-1}$) and CO_2 uptake capacity at 273 K and 1 bar (181 $mg{\cdot}g^{-1}$); the best CO_2/N_2 (15/85) selectivity calculated by IAST at 273 K and 1 bar belongs to **C1M2-Al** (32.3). Moreover, the synthesis route exhibits cost-effective advantages, which are essential for scale-up preparation, thus showing great potential for clean energy applications.

Introduction

Recently, climatic warming due to the rapid consumption of fossil fuels and biomass has gradually produced disastrous consequences. How to effectively capture CO_2 has been a common topic among the global scientific community.[1] The conventional CO_2 capture process based on alkanolamine solvents has significant drawbacks such as high energy consumption, corrosion of equipment and some environmental issues. In order to solve those problems, the new generation CO_2 capture technologies must be developed on a global scale.[2] Porous materials relying on physical adsorption are potential candidates for CO_2 capture because of their low regeneration energy consumption, high CO_2 sorption capacity and synthetic diversification.[3] Microporous organic polymers (MOPs) are an important class of porous materials which are constructed from monomers as organic building blocks and have shown great potential in a variety of applications, such as gas storage and separation, catalysis, chemical sensing, etc.[4] MOPs is a wide concept[5] which includes polymers of intrinsic microporosity (PIMs),[6] conjugated microporous polymers (CMPs),[7] covalent organic frameworks (COFs),[8] hyper-cross-linked polymers (HCPs),[9] crystalline triazine-based frameworks (CTFs),[10] porous polymer networks (PPNs)[11] and porous aromatic frameworks (PAFs).[12] However, most MOPs were obtained via cross-coupling reactions catalysed by precious metal catalysts, which limited their practical applications.

HCPs with high microporosity is a subclass of MOPs, which were prepared by Friedel-Crafts alkylation reaction in the presence of cheap, readily available Lewis acids as catalysts. They have the advantages of low production cost and easy scale production. There are two common approaches through Friedel-Crafts reaction to synthesize HCPs: one is direct polymerization of monomers, and the other one is intermolecular and intramolecular post crosslinking of preformed polymer chains.[13] Efforts made to explore such new hyper-cross-linked materials have achieved well-pleasing fruit. Some of these polymers featured great capability in carbon-capture. For example, Cooper's group reported an alcohol-containing polymer network with a significantly higher CO_2 uptake of 174 $mg{\cdot}g^{-1}$ at 1 bar and 273 K.[13c] Recently, Dai's group reported a new triazine and carbazole bifunctionalized task-specific polymer whose CO_2 uptake of 180 $mg{\cdot}g^{-1}$ at 1 bar and 273 K is among the highest uptake in porous HCPs.[14] Experimental results indicate that the innate abilities of the porous HCPs for the gas storage or separation are correlated to their pore structure including specific surface area, pore geometry, pore volume and pore size distribution. The Brunauer-Emmett-Teller (BET) specific surface area is a very important parameter in the pore structure for the HCPs, which can be tuned in the range of 300-2090 $m^2{\cdot}g^{-1}$ by manipulating the structure of the monomers and/or reaction parameters.[13h] Therefore, designing monomer and optimizing the synthetic condition to synthesize HCPs with higher specific surface areas are critical for the applications such as gas storage or separation.

In the classical Friedel-Crafts alkylation reaction, benzyl bromides could also be used as alkylating agents and the small

gases adsorptive property of the polymers resulting from tritopic benzyl bromides have never been systematically investigated. In addition, almost all the HCPs were carried out by using anhydrous $FeCl_3$ as catalyst.[13h] However, we found that the gas sorption properties of the polymers were largely affected by the structure of the polymers which were relevant to the activity of the reaction catalyst. Here we demonstrate that 1,3,5-tris(bromomethyl)benzene (**C1**) and 1,3,5-tris(bromomethyl)-2,4,6-trimehylbenzene) (**C2**) are firstly used as cross-linkers and co-condensed with ordinary aromatic compounds of different sizes to construct a series of cost-effective porous materials in the presence of anhydrous $FeCl_3$ or $AlCl_3$ as catalysts. The adsorption of CO_2 and H_2 as well as the separation of CO_2/N_2 were evaluated and compared in order to deeply study the effect of catalyst and building block features on the pore structures and the properties of target frameworks.

Experimental Section

Materials

Reagents and solvents were purchased from commercial suppliers and used without further purification, unless otherwise indicated. Dichloromethane (DCM) was dried by activated molecular sieve. 1,3,5-Tris(bromomethyl)benzene and 1,3,5-Tris(bromomethyl)-2,4,6-trimehylbenzene were synthesized following the published procedures.[15]

Synthesis of hyper−cross−linked porous polymers

All the microporous organic polymer networks were synthesized by Friedel-Crafts alkylation of benzene, biphenyl, or 1,3,5-triphenylbenzene using 1,3,5-tris(bromomethyl)-2,4,6-trimehylbenzene or 1,3,5-tris(bromomethyl)benzene as cross-linker promoted by anhydrous $AlCl_3$ or $FeCl_3$ in similar procedures. The preparation of sample **C1M1-Al** will serve as an example: $AlCl_3$ (anhydrous 500 mg, 3.75 mmol), 1,3,5-tris(bromomethyl)benzene(180 mg, 0.5 mmol) and benzene (60 mg, 0.75 mmol) were added to a 100 ml flask, and then 20 ml dry DCM was added to it. The mixture was stirred under nitrogen protection at 40 °C for 24 h to form the network. The colour of the mixture darkens with time. The resulting precipitate was washed three times with diluted hydrochloric acid, methanol, DCM and acetone, respectively, and then extracted by methanol in a Soxhlet for 24 h, and finally dried under reduced pressure at 160 °C for 24 h for further tests. Elemental analysis (%) Calcd. for $(C_{36}H_{30})_n$: C 93.46, H 6.54 (based on the 3.0 mmol starting material of benzene completely reacted with 2.0 mmol **C1**); found: C 81.56, H 5.71.

The same procedure was followed for the synthesis of other HCPs (Table 2) and the C, H elemental analysis data for all polymers are listed in Table 1. The deviations between calculated and found values are expected for such polymers due to incomplete combustion and trapped adsorbates including catalyst, gases and water vapour within the pore structure, which are consistent with the literature reported.[9b, 13e, 13i, 16]

Table 1 Elemental analysis data of the polymers.

Materials	Calculated (%)		Found (%)	
	C	H	C	H
C1M1-Al $(C_{36}H_{30})_n$	93.46	6.54	81.56	5.71
C1M2-Al $(C_{54}H_{42})_n$	93.87	6.13	88.60	5.50
C1M3-Al $(C_{33}H_{24})_n$	94.25	5.75	88.46	5.49
C2M1-Al $(C_{42}H_{42})_n$	92.26	7.74	86.20	6.46
C2M2-Al $(C_{60}H_{54})_n$	92.98	7.02	89.40	6.03
C2M3-Al $(C_{36}H_{30})_n$	93.46	6.54	88.46	5.88
C1M3-Fe $(C_{33}H_{24})_n$	94.25	5.75	64.88	3.68
C2M3-Fe $(C_{36}H_{30})_n$	93.46	6.54	70.86	4.58

Physical characterization

Fourier transform infrared (FT-IR) spectra of the MOPs were recorded on KBr pellets in the 4000−400 cm^{-1} range using a Perkin−Elmer Spectrum One FT-IR spectrometer. Elemental analyses (C, H, and N) were performed on an Elementar Vario MICRO elemental analyzer. Solid-state ^{13}C CP/MAS NMR were performed on a Bruker SB Avance III 500 MHz spectrometer with a 4-mm double-resonance MAS probe, a sample spinning rate of 9.0 kHz, a contact time of 2 ms and pulse delay of 5 s. A recycling delay of 10 s was used and 4096 scans were typically acquired for each spectrum. Thermal gravimetric analysis data were obtained with a NETZSCH STA 449C analyzer. All samples and reference (Al_2O_3) were enclosed in a platinum crucible and were heated from 25 °C to 1000 °C at a rate of 10 °C min^{-1} under a N_2 atmosphere. Powder X-ray diffraction (PXRD) patterns were collected on a Rigaku-D_{MAX} 2500 diffractometer with Cu Kα radiation (λ=1.5406 Å) at a scanning rate of 1° /min for 2θ ranging from 5° to 60°. Scanning Electron Microscopy (SEM) experiments were carried on a JSM 6700 at 10.0 kV. EDS was performed using a JSM 6700 microscope. Before measurement, the samples were sputter-coated with gold to facilitate conduction. Metal elemental analysis was carried out on an Ultima-2 ICP emission spectrometer. The textural properties of various sorbents were measured by N_2 sorption isotherms at 77 K using a Micromeritics ASAP 2020 surface area and porosimetry analyser. All samples were degassed at 160 °C for 24 h under conditions of dynamic vacuum before analysis. The specific surface areas for N_2 were calculated using the BET model over a relative pressure (P/P_0) range of 0.05 – 0.15. Total pore volumes were calculated from the uptake at a relative pressure of 0.995. Pore size distributions were calculated from the adsorption isotherms by no-local density functional theory (NLDFT) method. N_2 adsorption isotherm at 273 K was measured in order to evaluate the adsorption selectivity of CO_2/N_2. Hydrogen adsorption isotherms were measured on the ASAP 2020 at 77 K and 87 K up to 1.13 bar. Carbon dioxide adsorption isotherms were also collected on the ASAP 2020 at 273 K, 283 K and 298 K, respectively.

Results and Discussion

Synthesis and characterization of HCPs

We used 1,3,5-tris(bromomethyl)benzene (**C1**) and 1,3,5-tris(bromomethyl)-2,4,6-trimehylbenzene (**C2**) as 3-connected cross-linkers to construct a series of porous polymers. The polymers were readily obtained in good yields under mild reaction conditions by mixing cross-linker, monomer, catalyst, dry dichloride methane (DCM), and stirring at 40 °C for 24 h. The synthesis route for these polymer networks is present in Scheme 1. The resulting precipitate was fully washed three times with dilute hydrochloric acid, methanol, acetone and DCM, respectively. The product was purified through Soxhlet extractor in methanol for 24 h in order to remove all the remaining catalyst and monomer. The product was obtained as brownish power after dried under reduced pressure at 160 °C for 24 h.

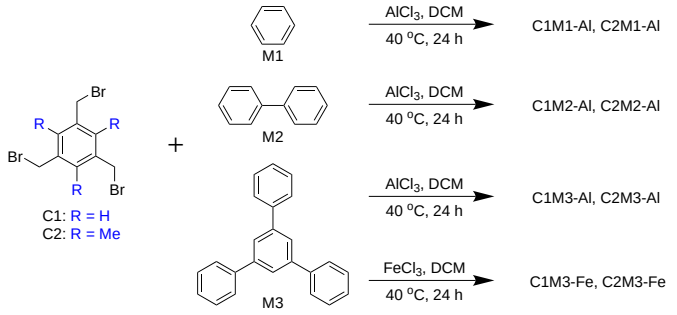

Scheme 1. Synthesis route for the HCPs

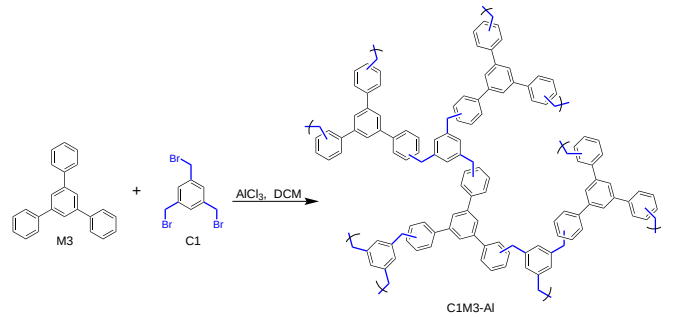

Scheme 2 Schematic presentation of the linkage (blue) between the monomers as well as the structure of the resulted polymers (**C1M3-Al** as an example)

We chose **C1** or **C2** as 3-connected building blocks and reacted with 1,3,5-triphenylbenzene (**M3**) in the presence of anhydrous $AlCl_3$ or $FeCl_3$, respectively, to evaluate the effect of catalysts on the structural features of the porous polymers. In addition, **C1** or **C2** were reacted with benzene (**M1**), biphenyl (**M2**), and 1,3,5-triphenylbenzene (**M3**), respectively, to afford six polymers under the catalysis of anhydrous $AlCl_3$ (Scheme 1 and 2).

Theoretically, each bromomethyl group should be converted into a methylene bridge by elimination of one hydrogen bromide molecule. But in fact, the residual bromine in the resulting polymers was found according to Energy Dispersive Spectrometer (EDS) (Table S1, Figure S1, ESI†), which indicates some bromomethyl groups may remain unsubstituted under the investigated reaction conditions. Similar results were also reported by other group with residual chlorine or oxygen in the HCPs.[5, 9a] Meanwhile, only relatively small amounts of residual iron or aluminium were found in all these networks (Table S2, ESI†), indicating that most of the catalysts were removed during the workup procedure.

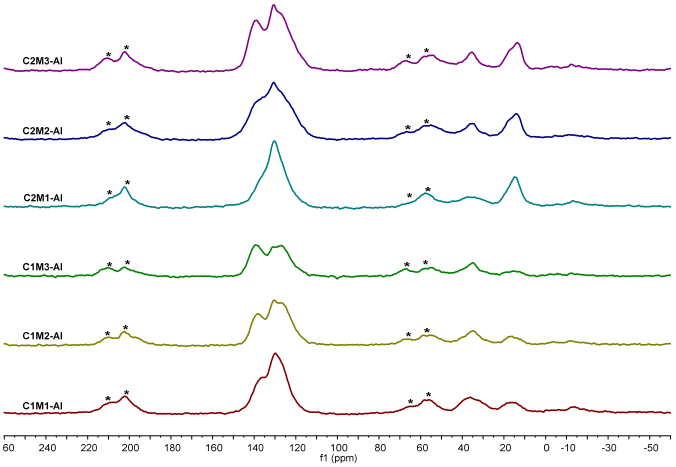

Fig. 1 Experimental ^{13}C CP-MAS NMR spectra of the polymer networks. Asterisks denote spinning sidebands.

The power X-ray diffraction measurement showed that all the samples were amorphous (Fig. S4, ESI†). The molecular details of the samples were confirmed by Fourier transform infrared (FTIR) spectroscopy, ^{13}C cross-polarization magic-angle spinning (CP/MAS) NMR and elemental analysis (EA). In the FTIR spectrum of all samples, peaks near 1600, 1500, and 1450 cm^{-1} were attributed to aromatic ring skeleton vibrations (Fig. S3, ESI†). The ^{13}C CP/MAS NMR of all tested samples are similar to the porous polymers obtained using formaldehyde dimethyl acetal (FDA) as cross-linker.[13b] The resonance peaks near 139 and 130 ppm can be easily ascribed to the substituted aromatic carbon and non-substituted aromatic carbon, respectively. All samples displayed methylene resonance peaks near 35 ppm, supporting the formation of methylene linker after Friedel-Crafts reaction and indicating the presence of the monomer moiety within the polymer network. **C2**-based polymers of **C2M1-Al**, **C2M2-Al** and **C2M3-Al** showed strong methyl resonance peaks near 16 ppm (Fig. 1). The resonance peaks of different samples revealed a little variation according to the character of the monomers and the knitting degree.

The morphology of the porous polymers was investigated by scanning electron microscopy (SEM). The SEM images revealed the formation of aggregated nanoparticles for all these polymers (Fig. S6-S13, ESI†). The materials were found to be stable in most common organic solvents and showed no degradation towards humidity. Further analyses of the polymers by thermal gravimetric analysis (TGA) showed that all the samples were stable up to 300 °C under nitrogen atmosphere and retained more than 60-85 % of their mass even at 1000 °C

(Fig. S2, ESI†), suggesting a good thermal stability due to the highly cross-linked network of the polymers.

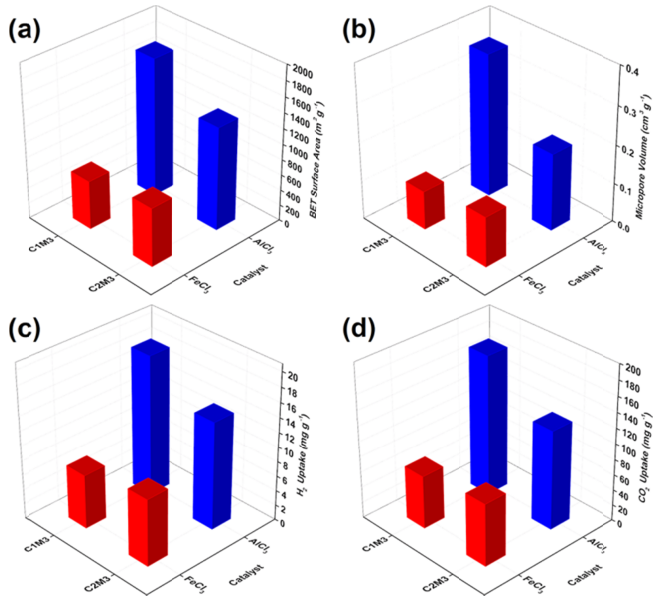

Fig. 2 The effects of the catalyst on porosity. (a) BET surface area. (b) micropore volume. (c) H_2 uptake at 77 K and 1 bar. (d) CO_2 uptake at 273 K and 1 bar.

Effect of catalyst on the porosity of HCPs

The Friedel-Crafts alkylation reaction can be catalysed by anhydrous $AlCl_3$, $FeCl_3$ or other Lewis acids. David C. Sherrington and his co-worker have explored the effect of the catalyst on the BET surface area of the resulting polymers and they found that $FeCl_3$ is a much more effective Lewis acid catalyst than $AlCl_3$ and $SnCl_4$.[13h] Influenced by this result, almost all of the following HCPs were synthesized by using anhydrous $FeCl_3$ as catalyst. However, the activities of catalyst are closely related to the different reactants and reaction conditions. In our case, the **C1M3** and **C2M3** were selected to carry on a performance contrast experiment of anhydrous $AlCl_3$ or $FeCl_3$. The result showed that the two catalysts had no substantial difference in synthetic efficiency. However, the porosity of samples catalysed by $AlCl_3$ outperformed that of samples catalysed by $FeCl_3$. Fig. 2 clearly demonstrates that the BET surface areas, micropove volume, H_2 uptake and CO_2 uptake of the polymers with anhydrous $AlCl_3$ as catalyst are significantly superior to those with anhydrous $FeCl_3$ as catalyst. It is not entirely clear why such significant differences arise between these species, however it may be that anhydrous $AlCl_3$ is the more powerful and common used catalyst than anhydrous $FeCl_3$.[17] The resulting polymers in the presence of $AlCl_3$ show a higher polymerization degree with the conversion of more CH_2Br groups into methylene bridges, which confirmed by element analysis (high C and H contents) and EDS (low Br content). The networks with higher degrees of condensation are less able to collapse and densify, thus leading to higher levels of microporosity.[9b] Considering the better porosity, we may conclude that anhydrous $AlCl_3$ is a much effective catalyst than anhydrous $FeCl_3$. As a result, anhydrous $AlCl_3$ was chosen as the catalyst in the following polymers synthesis.

View Article Online
DOI: 10.1039/C4TA05349D

Porosity and gas sorption studies

Permanent porosity was retained as expected even though removing the solvent, owing to numerous rigid knitting points preventing the framework collapse of the material. The surface area and porosity parameters of the samples were analysed by standard nitrogen sorption analysis at 77 K. As shown in Fig. 3, these porous polymers display a Type I isotherm with type IV character at higher relative pressures. The adsorption isotherms are characterized by a steep nitrogen gas uptake at low relative pressure ($P/P_0<0.1$), indicating permanent microporosity of all tested samples. The **C2**-based samples show different degree of hysteresis loop indicating partial mesoporosity. The gradual increase of nitrogen adsorption of the polymers at medium and high pressure region ($P/P_0=0.8$-1.0) indicates the presence of macroporous structure which can be interpreted as loose packing induced by inter-particulate voids in these materials. A small hysteresis is observed in the whole pressure range of desorption for all samples, which is consistent with the swelling effect as a result of gas sorption.[18]

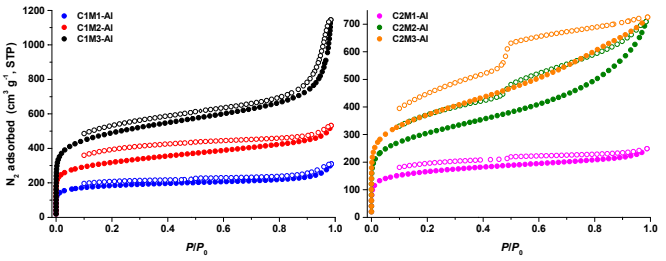

Fig. 3 N_2 sorption isotherms of the **C1MX-Al** and **C2MX-Al** (X = 1, 2 ,3) at 77 K (filled, adsorption; open, desorption).

The characterization of pore structure including surface area and the pore volume and gas sorption for these porous polymers are summarized in Table 2. The BET method was applied to determine the surface areas of these samples. As there are macropores in these polymers, the selection of isotherm points for BET surface area calculations had to be subjected to the values of $V(P_0-P)$ which increased continuously with P/P_0 in addition to a linear BET plot and a positive value of the c parameter (Fig. S14-S21, ESI†). The BET surface areas are in the range of 609 to 1783 $m^2 \cdot g^{-1}$ for this series. It is interesting to note that the BET surface area of the polymers based on the same cross-linker dramatically increase (from 688 $m^2 \cdot g^{-1}$ of **C1M1-Al**, 1164 $m^2 \cdot g^{-1}$ of **C1M2-Al** to 1783 $m^2 \cdot g^{-1}$ of **C1M3-Al**) when the size of the monomer increase. This trend is different from which obtained by Tan's group.[13b] Their research showed that benzene-based rather than **M3**-based network using FDA as cross-linker had the highest BET surface area, which was high up to 1391 $m^2 \cdot g^{-1}$. When the $AlCl_3$ was used as catalyst, the polymers based on C1 showed higher surface area compared to the polymers based on C2. However, the polymers of $FeCl_3$-catalyzed did not follow this trend and C2 based polymer showed ~20% higher specific surface area (Table 2),

which reflected the significant difference between $AlCl_3$ and $FeCl_3$ as catalyst in this case. These data further highlight the fact that the porous properties of the resulting polymers are synthetically affected by the nature of monomers and catalyst.

The highest BET surface area (1783 $m^2 \cdot g^{-1}$) and pore volume (1.29 $cm^3 \cdot g^{-1}$) were obtained for **C1M3-Al**. The results of our work can be comparable to or higher than that of other HCPs produced by Friedel-Crafts alkylation (Table 3). The porosity in these polymers is controlled not only by the level of cross-linking but also by subtle changes in the design of the rigid monomer units.

Pore size distribution (PSD) for these polymers was calculated using nonlocal density functional theory (NLDFT), indicating that these networks are filled with a significant fraction of micropore less than 10 Å in size (Fig. S5, ESI†). Previous studies suggest that only pores less than 10 Å are proved to be effective for H_2 storage or CO_2 capture at low pressure since the kinetic diameters of H_2 and CO_2 are 2.9 and 3.3 Å, respectively.[9b, 16, 19] Thus, an expected excellent adsorption performance may be achieved for these materials, which inspired us to further study the H_2 and CO_2 uptake abilities of these polymers.

Table 2 Synthetic condition, surface area and pore volume and gas sorption properties of this series.

Materials	Crosslinker mmol	Monomer mmol	SA_{BET} $m^2 \cdot g^{-1}$	V_{Total}[a] $cm^3 \cdot g^{-1}$	V_{Micro}[b] $cm^3 \cdot g^{-1}$	CO_2 uptake[c]		H_2 uptake[d]		CO_2/N_2 Selectivity[e]
						$mg \cdot g^{-1}$	Q_{st} $kJ \cdot mol^{-1}$	$mg \cdot g^{-1}$	Q_{st} $kJ \cdot mol^{-1}$	
C1M1-Al	**C1** (0.5)	Benzene (0.75)	688	0.40	0.19	101		8.0		
C2M1-Al	**C2** (0.5)	Benzene (0.75)	609	0.35	0.14	63.6		7.2		
C1M2-Al	**C1** (0.5)	Biphenyl (0.75)	1164	0.73	0.26	150	22.3	14.5	8.5	32.3
C2M2-Al	**C2** (0.5)	Biphenyl (0.75)	1103	0.98	0.17	112	20.6	12.1	9.1	27.7
C1M3-Al	**C1** (0.5)	TPB (0.5)	1783	1.29	0.37	181	20.9	19.1	7.9	23.4
C2M3-Al	**C2** (0.5)	TPB (0.5)	1342	1.06	0.20	128	20.1	14.6	8.1	24.9
C1M3-Fe	**C1** (0.5)	TPB (0.5)	628	0.62	0.10	67.7		7.3		
C2M3-Fe	**C2** (0.5)	TPB (0.5)	755	0.66	0.13	79.9		9.0		

[a]Pore volume calculated from N_2 isotherm at P/P_0= 0.95 and 77 K. [b]Micropore volume calculated from t-Plot method. [c]273 K and 1 bar. [d]77 K and 1 bar. [e] IAST-predicted adsorption selectivities at 273 K and 1 bar using a 15:85 CO_2:N_2 ratio.

Table 3 Summary of the gas-uptake capacities of various HCPs for H_2 and CO_2 at low pressure.

Monomer \ Cross-linker	S_{BET} m^2 g^{-1}	H_2 uptake[a] mg g^{-1}	CO_2 uptake[b] mg g^{-1}	Ref
TPB[c] / C1	1783	19.1	181	this work
TCT[d] / FDA[e]	913	-	180	14
TPB / FDA	1059	15.8[f]	159	13b
1,1'-bi-2-naphthol / FDA	1015	-	174	13c
fluorene / BCMBP[g]	1700	16.3	-	13a
TPE[h] / FDA	1980	17.6	160	13e
benzene / FDA	1391	14.5[f]	135	13b
TPM[i] / FDA	1470	-	130	20

[a]77 K and 1 bar. [b]273 K and 1 bar. [c]TPB: 1,3,5-triphenylbenzene. [d]TCT: 2,4,6-Tricarbazolo-1,3,5-triazine. [e]FDA: formaldehyde dimethyl acetal. [f]1.13 bar. [g]BCMBP: 4,4'-bis(chloromethyl)biphenyl. [h]TPE: tetraphenylethylene. [i]TPM: tetraphenylmethane

A summary of the H_2 and CO_2 uptakes for the various porous polymers are presented in Fig. 4. All samples show significant H_2 uptake even though their surface areas are moderate, and no saturation was observed in the studied range of pressures and temperatures, which indicates that higher H_2 capacity can be achieved by increasing the pressure above 1 bar. The CO_2 uptake of **C1M3-Al** is up to 181 $mg \cdot g^{-1}$ at 1 bar and 273 K, which is comparable to that of **BILP**-10 (177 mg g^{-1}),[21] OH functionalized porous organic frameworks (183 mg g^{-1}),[22] and other polymer networks.[23] To the best of our knowledge, the adsorption capacities of **C1M3-Al** for CO_2 and H_2 is the highest in the HCPs under similar conditions reported so far (Table 3). These data prove that specific surface area, molecular structure and chemical character of the resulting porous polymers should be optimized in a synergistic way in order to enhance the gas uptake capacity. In general, increased gas uptake capacities were observed with increased surface area, i.e., CO_2 and H_2 uptakes at 1 bar follow the order of surface areas of these polymer networks when same cross–linker used: **C1M3-Al**>**C1M2-Al**>**C1M1-Al**. The CO_2 and H_2 uptake properties of **C1**-based polymers are better than **C2**-based polymers when the same monomer was used. For example, **C2M3-Al** has lower H_2 and CO_2 uptake capacities than **C1M3-Al**.

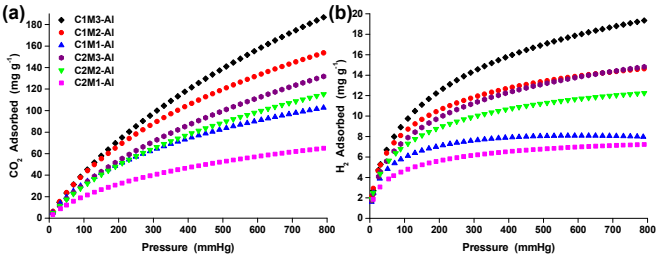

Fig. 4. Small gas adsorption of the samples at low pressure. (a) CO_2 adsorption isotherms at 273 K; (b) H_2 adsorption isotherms at 77 K.

Isosteric heat of adsorption of CO_2 and H_2

To provide a further understanding of the binding affinity of the studied porous polymers toward CO_2, the isosteric heat of

adsorption (Q_{st}) was also calculated from the CO_2 isotherms measured at 273, 283 and 293 K. The calculated Q_{st} values at the initial adsorption stage for **C1M2-Al**, **C2M2-Al**, **C1M3-Al** and **C2M3-Al** are on the scale of 20.1-22.3 kJ·mol^{-1} (Table 1), which are comparable to other HCPs (20-24 kJ·mol^{-1}),[9b] BLPs(20.2-28.3 kJ·mol^{-1}),[24] while lower than those microporous polymers decorated with functional groups.[11c, 25] The values remain well below the energy of the chemical bond suggesting the polymers interact moderately with CO_2 molecules which is desirable for the regeneration of adsorbents. The isotherms exhibit relatively steep initial uptakes at low pressures which indicates a strong affinity towards H_2 gas. The H_2 Q_{st} values were also calculated from the H_2 isotherms measured at 77 K and 87 K (Table 1, Fig. 5). At the onset of adsorption, the H_2 Q_{st} values are 8.5, 9.1, 7.9 and 8.1 kJ·mol^{-1} for **C1M2-Al**, **C2M2-Al**, **C1M3-Al** and **C2M3-Al**, respectively, which are higher than other organic polymers such as porous polymer networks (PPNs, 5.5-7.6 kJ·mol^{-1}),[11a] polyimide networks (5.3-7.0 kJ mol^{-1})[26] and nitrogen rich porous aromatic frameworks (NPAF, 5.2 kJ mol^{-1}).[27] The H_2 Q_{st} of the polymers based on **C2** are higher than that of the polymers based on **C1** when same monomer used, which indicates that the introduction of methyl group narrow the pores and thus strengthen the interaction between H_2 and polymers.

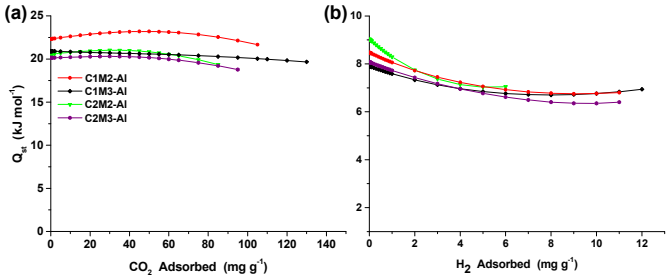

Fig. 5 Plots of the isosteric heat of adsorption (Qst) for CO_2 and H_2

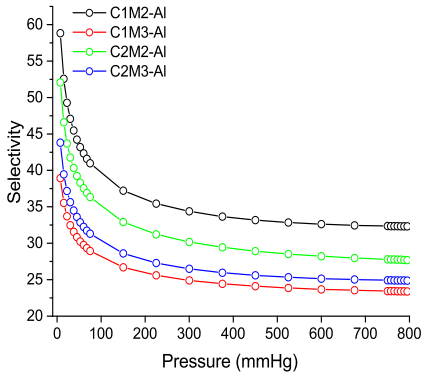

Fig. 6 IAST selectivities of CO_2 over N_2 for binary gas mixtures of 15/85 molar composition at 273 K

Gas selectivity studies

The above results indicate that these porous polymers possess the excellent CO_2 uptake abilities, which motivate us to further investigate the gas selectivity of these networks. N_2 adsorption experiments of four selected samples with high CO_2 uptake were carried out at 1 bar to examine the separation capability. The single-component gas sorption experiments were first carried out on CO_2 and N_2 at 273 K and pressured up to 1 bar. The CO_2 and N_2 isotherms of all the tested samples show no isotherm inflection and are fitting by the single-site Langmuir-Freundlich equation to get equilibrium parameters, saturation capacities and Langmuir constants. The CO_2/N_2 selectivity was predicted using ideal adsorption solution theory (IAST), which has frequently been used to predict the behaviour of mixed component isotherms based on single component isotherms. The IAST calculations were carried out for binary mixture containing 15% CO_2 and 85% N_2 in the typical flue gases, and the results are shown in Fig. 6 and the selectivities of the polymers for CO_2/N_2 at 1 bar and 273 K was given in Table 1. As shown in Fig. 6, the CO_2/N_2 selectivities of the four samples at 273 K decrease slowly as pressure increase. It is interesting that the **C1M2-Al** in the four samples shows the highest CO_2/N_2 selectivity (32.3 at 1 bar and 273 K), which is higher than PPFs (14.5-20.4),[28] FCTF-1 (31)[29] and NPOF-4 (12),[30] but lower than those functionalized porous organic frameworks.[11c, 31] In our case, the high BET surface area has not led to the high CO_2/N_2 selectivity, which indicates that CO_2/N_2 selectivity is influenced by a combination of factors of pore structure. An ideal adsorbent should be capable of adsorbing a large amount of CO_2 with a high CO_2/N_2 selectivity at low CO_2 partial pressures (< 0.2 bar). Among these polymers, **C1M2-Al** is the good candidate for the balanced CO_2 uptake capacity and CO_2/N_2 selectivity.

Conclusions

We have successfully synthesized a series of porous polymer frameworks with two different tritopic benzyl bromide cross-linkers and different aromatic monomers through the Friedel−Crafts alkylation. The catalyst effect for the pore structure has been re-evaluated. A comparative study of gas uptake ability shows that the anhydrous $AlCl_3$ is a much more effective Lewis acid catalyst than anhydrous $FeCl_3$ and is more beneficial in terms of porosity and gas sorption. The BET surface area of these polymers is up to 1783 m^2g^{-1}. As expected, these polymers exhibit exceptionally high H_2 uptake of up to 19.1 mg·g^{-1} (77 K and 1 bar), and high CO_2 uptake of 181 mg·g^{-1} (273 K and 1 bar), which are among the highest reported values for HCPs under the same conditions. These polymers also exhibit excellent CO_2 sorption selectivity, the best CO_2/N_2 (15/85) selectivity calculated by IAST at 273 K and 1 bar is up to 32.3 for **C1M2-Al**. In our case, the gas sorption properties depend on the nature of the cross-linker used. Due to the inexpensive starting material, the preparative strategy exhibits cost-effective advantages and these porous polymers are promising candidates for energy applications on a larger scale.

Acknowledgements

This work was supported by the NSFC (Grants 21271172 and 21131006), the "One Hundred Talent Project" from Chinese Academy of Sciences, and the NSF of Fujian Province (Grant 2012J01058)

Notes and references

[a] State Key Laboratory of Structural Chemistry, Fujian Institute of Research on the Structure of Matter, Chinese Academy of Sciences, Fuzhou, Fujian 350002 (P. R. China). E-mail: ydq@fjirsm.ac.cn

[b] University of Chinese Academy of Sciences, Beijing 100049 (P. R. China).

† Electronic Supplementary Information (ESI) available: Synthesis and Characterization data. See DOI: 10.1039/b000000x/

1. (a) K. Sumida, D. L. Rogow, J. A. Mason, T. M. McDonald, E. D. Bloch, Z. R. Herm, T. H. Bae and J. R. Long, *Chem. Rev.*, 2012, **112**, 724; (b) Z. Chang, D. S. Zhang, Q. Chen and X. H. Bu, *Phys. Chem. Chem. Phys.*, 2013, **15**, 5430; (c) S. Xu, Y. Luo and B. Tan, *Macromol. Rapid Commun.*, 2013, **34**, 471; (d) S. Enthaler, *ChemSusChem*, 2008, **1**, 801; (e) K. M. Yu, I. Curcic, J. Gabriel and S. C. Tsang, *ChemSusChem*, 2008, **1**, 893.
2. (a) G. T. Rochelle, *Science*, 2009, **325**, 1652; (b) N. MacDowell, N. Florin, A. Buchard, J. Hallett, A. Galindo, G. Jackson, C. S. Adjiman, C. K. Williams, N. Shah and P. Fennell, *Energy Environ. Sci.*, 2010, **3**, 1645; (c) D. M. D'Alessandro, B. Smit and J. R. Long, *Angew. Chem. Int. Ed.*, 2010, **49**, 6058.
3. (a) S. Choi, J. H. Drese and C. W. Jones, *ChemSusChem*, 2009, **2**, 796; (b) A. Goeppert, H. Zhang, M. Czaun, R. B. May, G. K. Prakash, G. A. Olah and S. R. Narayanan, *ChemSusChem*, 2014, **7**, 1386; (c) Y. Hu, W. M. Verdegaal, S. H. Yu and H. L. Jiang, *ChemSusChem*, 2014, **7**, 734.
4. (a) R. Dawson, A. I. Cooper and D. J. Adams, *Prog. Polym. Sci.*, 2012, **37**, 530; (b) J.-X. Jiang and A. I. Cooper, *Top. Curr. Chem.*, 2010, **293**, 1.
5. Y. L. Luo, S. C. Zhang, Y. X. Ma, W. Wang and B. Tan, *Polym. Chem.*, 2013, **4**, 1126.
6. (a) N. B. McKeown, P. M. Budd, K. J. Msayib, B. S. Ghanem, H. J. Kingston, C. E. Tattershall, S. Makhseed, K. J. Reynolds and D. Fritsch, *Chem. Eur. J.*, 2005, **11**, 2610; (b) N. B. McKeown, B. Gahnem, K. J. Msayib, P. M. Budd, C. E. Tattershall, K. Mahmood, S. Tan, D. Book, H. W. Langmi and A. Walton, *Angew. Chem. Int. Ed.*, 2006, **45**, 1804; (c) B. S. Ghanem, K. J. Msayib, N. B. McKeown, K. D. Harris, Z. Pan, P. M. Budd, A. Butler, J. Selbie, D. Book and A. Walton, *Chem. Commun.*, 2007, 67.
7. J. X. Jiang, F. Su, A. Trewin, C. D. Wood, N. L. Campbell, H. Niu, C. Dickinson, A. Y. Ganin, M. J. Rosseinsky, Y. Z. Khimyak and A. I. Cooper, *Angew. Chem. Int. Ed.*, 2007, **46**, 8574.
8. (a) H. M. El-Kaderi, J. R. Hunt, J. L. Mendoza-Cortes, A. P. Cote, R. E. Taylor, M. O'Keeffe and O. M. Yaghi, *Science*, 2007, **316**, 268; (b) F. J. Uribe-Romo, C. J. Doonan, H. Furukawa, K. Oisaki and O. M. Yaghi, *J. Am. Chem. Soc.*, 2011, **133**, 11478.
9. (a) C. D. Wood, B. Tan, A. Trewin, H. Niu, D. Bradshaw, M. J. Rosseinsky, Y. Z. Khimyak, N. L. Campbell, R. Kirk, E. Stockel and A. I. Cooper, *Chem. Mater.*, 2007, **19**, 2034; (b) C. F. Martín, E. Stöckel, R. Clowes, D. J. Adams, A. I. Cooper, J. J. Pis, F. Rubiera and C. Pevida, *J. Mater. Chem.*, 2011, **21**, 5475; (c) S. Xu, K. Song, T. Li and B. Tan, *J. Mater. Chem. A*, 2014, DOI: 10.1039/c4ta05265j.
10. (a) P. Kuhn, M. Antonietti and A. Thomas, *Angew. Chem. Int. Ed.*, 2008, **47**, 3450; (b) M. J. Bojdys, J. Jeromenok, A. Thomas and M. Antonietti, *Adv. Mater.*, 2010, **22**, 2202; (c) M. X. Tan, Y. Zhang and J. Y. Ying, *ChemSusChem*, 2013, **6**, 1186.
11. (a) W. Lu, D. Yuan, D. Zhao, C. I. Schilling, O. Plietzsch, T. Muller, S. Bräse, J. Guenther, J. Blümel, R. Krishna, Z. Li and H.-C. Zhou, *Chem. Mater.*, 2010, **22**, 5964; (b) D. Yuan, W. Lu, D. Zhao and H. C. Zhou, *Adv. Mater.*, 2011, **23**, 3723; (c) W. Lu, D. Yuan, J. Sculley, D. Zhao, R. Krishna and H.-C. Zhou, *J. Am. Chem. Soc.*, 2011, **133**, 18126.
12. (a) T. Ben, H. Ren, S. Ma, D. Cao, J. Lan, X. Jing, W. Wang, J. Xu, F. Deng, J. M. Simmons, S. Qiu and G. Zhu, *Angew. Chem. Int. Ed.*, 2009, **48**, 9457; (b) C. Zhang, L.-H. Peng, B. Li, Y. Liu, P.-C. Zhu, Z. Wang, D.-H. Zhan, B. Tan, X.-L. Yang and H.-B. Xu, *Polym. Chem.*, 2013, **4**, 3663.
13. (a) M. G. Schwab, A. Lennert, J. Pahnke, G. Jonschker, M. Koch, I. Senkovska, M. Rehahn and S. Kaskel, *J. Mater. Chem.*, 2011, **21**, 2131; (b) B. Li, R. Gong, W. Wang, X. Huang, W. Zhang, H. Li, C. Hu and B. Tan, *Macromolecules*, 2011, **44**, 2410; (c) R. Dawson, L. A. Stevens, T. C. Drage, C. E. Snape, M. W. Smith, D. J. Adams and A. I. Cooper, *J. Am. Chem. Soc.*, 2012, **134**, 10741; (d) X. F. Jing, D. L. Zou, P. Cui, H. Ren and G. S. Zhu, *J. Mater. Chem. A*, 2013, **1**, 13926; (e) S. W. Yao, X. Yang, M. Yu, Y. H. Zhang and J. X. Jiang, *J. Mater. Chem. A*, 2014, **2**, 8054; (f) J. Y. Lee, C. D. Wood, D. Bradshaw, M. J. Rosseinsky and A. I. Cooper, *Chem. Commun.*, 2006, 2670; (g) M. G. Schwab, I. Senkovska, M. Rose, N. Klein, M. Koch, J. Pahnke, G. Jonschker, B. Schmitz, M. Hirscher and S. Kaskel, *Soft Matter*, 2009, **5**, 1055; (h) J.-H. Ahn, J.-E. Jang, C.-G. Oh, S.-K. Ihm, J. Cortez and D. C. Sherrington, *Macromolecules*, 2006, **39**, 627; (i) R. Dawson, T. Ratvijitvech, M. Corker, A. Laybourn, Y. Z. Khimyak, A. I. Cooper and D. J. Adams, *Polym. Chem.*, 2012, **3**, 2034.
14. X. Zhu, S. M. Mahurin, S. H. An, C. L. Do-Thanh, C. Tian, Y. Li, L. W. Gill, E. W. Hagaman, Z. Bian, J. H. Zhou, J. Hu, H. Liu and S. Dai, *Chem. Commun.*, 2014, **50**, 7933.
15. (a) C. A. Ilioudis, D. A. Tocher and J. W. Steed, *J. Am. Chem. Soc.*, 2004, **126**, 12395; (b) A. W. van der Made and R. H. van der Made, *J. Org. Chem.*, 1993, **58**, 1262.
16. Y. Liu, S. Wu, G. Wang, G. Yu, J. Guan, C. Pan and Z. Wang, *J. Mater. Chem. A*, 2014, **2**, 7795.
17. (a) W. Chaikittisilp, M. Kubo, T. Moteki, A. Sugawara-Narutaki, A. Shimojima and T. Okubo, *J. Am. Chem. Soc.*, 2011, **133**, 13832; (b) M. B. Smith and J. March, in *March's Advanced Organic Chemistry*, John Wiley & Sons, Inc., 2006, 729.
18. J. Weber, M. Antonietti and A. Thomas, *Macromolecules*, 2008, **41**, 2880.
19. J. A.-M. D. Cazorla-Amorós, and A. Linares-Solano, *Langmuir*, 1996, **12**, 2820.
20. R. Dawson, E. Stöckel, J. R. Holst, D. J. Adams and A. I. Cooper, *Energy Environ. Sci.*, 2011, **4**, 4239.
21. M. G. Rabbani, A. K. Sekizkardes, O. M. El-Kadri, B. R. Kaafarani and H. M. El-Kaderi, *J. Mater. Chem.*, 2012, **22**, 25409.
22. A. P. Katsoulidis and M. G. Kanatzidis, *Chem. Mater.*, 2011, **23**, 1818.

View Article Online
DOI: 10.1039/C4TA05349D

23. (a) G. Li and Z. Wang, *Macromolecules*, 2013, **46**, 3058; (b) S. Wu, S. Gu, A.-Q. Zhang, G. Yu, Z. Wang, c. Pan and X. Jian, *J. Mater. Chem. A*, 2014, DOI: 10.1039/c4ta04734f.
24. (a) K. T. Jackson, M. G. Rabbani, T. E. Reich and H. M. El-Kaderi, *Polym. Chem.*, 2011, **2**, 2775; (b) T. E. Reich, S. Behera, K. T. Jackson, P. Jena and H. M. El-Kaderi, *J. Mater. Chem.*, 2012, **22**, 13524.
25. R. Dawson, D. J. Adams and A. I. Cooper, *Chem. Sci.*, 2011, **2**, 1173.
26. Z. Wang, B. Zhang, H. Yu, L. Sun, C. Jiao and W. Liu, *Chem. Commun.*, 2010, **46**, 7730.
27. D. E. Demirocak, M. K. Ram, S. S. Srinivasan, D. Y. Goswami and E. K. Stefanakos, *J. Mater. Chem. A*, 2013, **1**, 13800.
28. Y. Zhu, H. Long and W. Zhang, *Chem. Mater.*, 2013, **25**, 1630.
29. Y. Zhao, K. X. Yao, B. Teng, T. Zhang and Y. Han, *Energy Environ. Sci.*, 2013, **6**, 3684.
30. T. İslamoğlu, M. Gulam Rabbani and H. M. El-Kaderi, *J. Mater. Chem. A*, 2013, **1**, 10259.
31. (a) W. Lu, J. P. Sculley, D. Yuan, R. Krishna, Z. Wei and H.-C. Zhou, *Angew. Chem. Int. Ed.*, 2012, **51**, 7480; (b) Z. Qiao, Z. Wang, S. Zhao, S. Yuan, J. Wang and S. Wang, *RSC Adv.*, 2013, **3**, 50; (c) H. A. Patel, S. Hyun Je, J. Park, D. P. Chen, Y. Jung, C. T. Yavuz and A. Coskun, *Nat. Commun.*, 2013, **4**, 1357.

View Article Online
DOI: 10.1039/C4TA05349D

TOC

A facile synthesis of microporous organic polymers for efficient gas storage and separation

Guoliang Liu,[a,b] Yangxin Wang,[a,b] Chaojun Shen,[a] Zhanfeng Ju[a] and Daqiang Yuan[*,a]

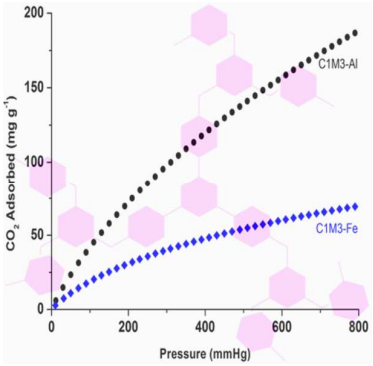

A series of porous polymers based on tritopic benzyl bromide exhibit high H_2 and CO_2 uptake capacities and CO_2/N_2 selectivities.